JBC Papers in Press. Published on March 13, 2017 as Manuscript M116.773788
The latest version is at http://www.jbc.org/cgi/doi/10.1074/jbc.M116.773788

A hot-spot on Interferon alpha/beta receptor subunit 1 (IFNAR1) underpins its interaction with Interferon-β and dictates signaling.

Nicole A de Weerd[1,2#], Antony Y Matthews[1,2], Phillip R Pattie[1], Nollaig M Bourke[1,2], San S Lim[1,2], Julian P Vivian[3,4], Jamie Rossjohn[3,4,5], Paul J Hertzog[1,2#]

Author affiliations:
[1] Centre for Innate Immunity and Infectious Diseases, Hudson Institute of Medical Research, 27-31 Wright Street, Clayton, Victoria 3168, Australia
[2] Department of Molecular and Translational Sciences, School of Clinical Sciences at Monash Health, Monash University, 27-31 Wright Street, Clayton, Victoria 3168, Australia
[3] Infection and Immunity Program & Department of Biochemistry and Molecular Biology, Biomedicine Discovery Institute, Monash University, Clayton, Victoria 3800, Australia
[4] Australian Research Council Centre of Excellence in Advanced Molecular Imaging, Monash University, Clayton, Victoria 3800, Australia
[5] Institute of Infection and Immunity, Cardiff University School of Medicine, Heath Park, Cardiff, CF14 4XN, United Kingdom

Running title: Hot-spot on IFNAR1 underpins IFN-β signaling

#To whom correspondence may be addressed: Dr. Nicole A. de Weerd, Centre for Innate Immunity and Infectious Diseases, Hudson Institute of Medical Research, Clayton, Victoria. Telephone (61) 3 85722760, Email: nicole.deweerd@hudson.org.au
#To whom correspondence may be addressed: Prof Paul J. Hertzog, Centre for Innate Immunity and Infectious Diseases, Hudson Institute of Medical Research, Clayton, Victoria. Telephone (61) 3 85722731, Email: paul.hertzog@hudson.org.au

Keywords: Interferon, receptor, structure-function, mutagenesis, signal transduction

ABSTRACT

The interaction of IFN-β with its receptor IFNAR1 is vital for host-protective anti-viral and anti-proliferative responses, but signaling via this interaction can be detrimental if dysregulated. While it is established that IFNAR1 is an essential component of the IFNAR signaling complex, the key residues underpinning the IFN-β-IFNAR1 interaction are unknown. Guided by the crystal structure of the IFN-β-IFNAR1 complex, we used truncation variants and site directed mutagenesis to investigate domains and residues enabling complexation of IFN-β to IFNAR1. We have identified an interface on IFNAR1-subdomain (SD)-3 that is differentially utilized by IFN-β and IFN-α for signal transduction. We used surface plasmon resonance and cell-based assays to investigate this important IFN-β binding interface which is centered on IFNAR1 residues Y^{240} and Y^{274} binding the C-terminal and N-terminal of B and C helices of IFN-β, respectively. Using IFNAR1 and IFN-β variants, we show that this interface contributes significantly to the affinity of IFN-β for IFNAR1, its ability to activate STAT1, the expression of interferon stimulated genes and ultimately to the anti-viral and anti-proliferative properties of IFN-β. These results identify a key interface created by IFNAR1 residues Y^{240} and Y^{274} interacting with IFN-β residues F^{63}, L^{64}, E^{77}, T^{78}, V^{81}, R^{82} that underlie IFN-β-IFNAR1 mediated signaling and biological processes.

The type I IFNs, including 14 IFN-α, and lone IFN-β, IFN-ε and IFN-ω, have critical roles in response to viral and bacterial infections, and cancers (1,2). They are also applied clinically for the treatment of hepatitis virus B and C (1), cancers including melanoma (3), and multiple sclerosis (4). Although they show clinical efficacy, their use is restricted by dose-limiting toxicities, including leukopenia, nausea, fatigue, neurological disorders (3), and localized cutaneous effects (5). All type I IFNs engage their cognate receptors, IFNAR1 and IFNAR2, to activate the canonical JAK-STAT signaling pathway, but ligand engagement can also activate alternative signaling pathways (6). Despite sharing these receptor components, there are IFN subtype-specific elements to signaling: compared to IFN-α, IFN-β has specific roles in osteoclastogenesis (7), control of chronic viral infection (8), the potent induction of apoptotic pathways required for control of tumor cell growth and the development of B cells and myelopoiesis (9).

Structural insight into the IFN-IFNAR interactions has been gleaned from the crystal structures of a human IFN-α2 variant and human IFN-ω in complex with both IFNAR1 and IFNAR2 (10). Furthermore, specific insight into the mode of IFN-β-mediated activation of IFNAR1 was obtained from the crystal structure of the murine IFN-β-IFNAR1 complex (11). Comparison of these structures and evidence form the literature (12) suggests that the minimal ligand binding domains for human and mouse IFNAR1 are similar, and sit broadly across the three membrane distal SDs (SD1-3) of the receptor with limited involvement of the membrane proximal subdomain, SD4 (Fig. 1A). It has also been shown that key residues discriminate between ligands and that there is potential for ligand-specific interaction interfaces (10,11). However experimental validation of these predictions is lacking.

The current study investigates the ligand-receptor subdomains and residues that contribute to the formation of a stable complex between IFN-β and the extracellular domain (ECD) of IFNAR1. Using subdomain truncation variants of IFNAR1-ECD we initially show that IFNAR1-SD3 is vital to the formation of a stable IFN-β-IFNAR1 complex. We next interrogated the crystal structure of the IFN-β-IFNAR1 complex, focusing on key residues on IFNAR1-SD3 and residues to which they interact on IFN-β. Our data reveals that a key interaction interface exists between two tyrosine residues on IFNAR1-SD3 and a small number of residues on IFN-β helices B and C. Using site directed mutagenesis we demonstrate that this interface is used differentially by IFN-β compared to IFN-α1. Furthermore, we show that this interface significantly influences the affinity of IFN-β for IFNAR1, the IFN-β-mediated internalization of IFNAR1, activation of STAT1 and the induction of interferon stimulated genes (ISGs). Importantly, we also show that this interface influences the magnitude of the biological activities that result from the IFN-β-IFNAR1 interaction.

RESULTS

The structural determination of murine IFNAR1 receptor in complex with IFN-β (PDB code 3WCY) revealed the interaction to be dominated by the three membrane-distal domains of the receptor with each contributing approximately a third of the binding interface (Fig. 1A). By contrast, the fourth domain of IFNAR1 contributed just 5% to the overall interface (Fig. 1A). We sought to understand the relative importance of IFNAR1 subdomains and individual IFN-β-IFNAR1 residues (Fig. 1B, C) to the formation of this high affinity complex, and the contributions these residues made to the functionality of IFN-β via IFNAR1.

IFNAR1-SD3 is vital for efficient IFN-β binding—To assess the relative importance of SDs of IFNAR1-ECD to IFN-β binding, we generated truncation variants of IFNAR1-ECD by introducing stop codons at the C-termini of SD3 (to generate IFNAR1-SD123) and of SD2 (to generate IFNAR1-SD12) (Fig. 1D). Using Native PAGE, we compared the ability of these truncated forms and the full length IFNAR1-ECD to bind IFN-β under native conditions. As we have previously shown, the addition of IFN-β induces an observable shift in mobility of IFNAR1-ECD (11). A similar observable shift in mobility was also seen with the addition of IFN-β to IFNAR1-SD123, indicating that IFN-β bound this truncated form of IFNAR1-ECD under these conditions (Fig. 1E). However, the addition of IFN-β to IFNAR1-SD12 did not alter the mobility of this form of IFNAR1-ECD, indicating that IFN-β did not bind this protein efficiently under these conditions (Fig. 1E). These data suggest that under native PAGE conditions the presence of SD3 of IFNAR1-ECD was critical for efficient binding of IFN-β.

Two residues, Y^{240} and Y^{274}, dominate the interaction interface on IFNAR1-ECD SD3—Examination of the contacts between IFNAR1-ECD and IFN-β in the crystal structure of the IFN-β-IFNAR1 complex revealed that central to the binding of IFNAR1-SD3 were the residues Y^{240} and Y^{274}. Using the AREA/MOL program from the CCP4 suite (13), we determined that these residues together contributed 40% of the total binding interface of this subdomain (Fig. 1B). Y^{240}, located on the loop between the β3 and β4 strands of IFNAR1-SD3, was pivotal to binding the C-terminal of the IFN-β B helix and N-terminal of the IFN-β C helix. Y^{240} sat in a predominantly hydrophobic pocket of IFNAR1-SD3 with principal interactions to IFN-β residues F^{63}, V^{81}, L^{84}, and H^{88} (Fig. 1C). IFNAR1 Y^{274}, located on the loop between the β5 and β6 strands of IFNAR1-SD3, was similarly pivotal to binding the N-terminal of the C helix of IFN-β and sat in a polar pocket characterized by a hydrogen bond to E^{77} and by van de Waals interactions with T^{78}, V^{81}, and R^{82} (Fig. 1C).

IFNAR1 residues Y^{240} and Y^{274} are important for IFN-β affinity—We expressed recombinant forms of IFNAR1-ECD containing mutations at Y^{240}, Y^{274} or both, generating IFNAR1-ECD Y240A, IFNAR1-ECD Y274A, and IFNAR1-ECD Y240A/Y274A (herein referred to as IFNAR1-ECD YYAA), respectively (Fig. 2A). We assessed the binding of IFN-β to these receptor variants using surface plasmon resonance (SPR). Our results show that while alanine substitutions at Y^{240} or Y^{274} showed slight but not statistically significant reductions in IFN-β binding (Table 1), a synergistic effect was observed when these two mutations were combined in IFNAR1-ECD YYAA. The affinity of IFN-β for IFNAR1-ECD YYAA was significantly reduced ~69-fold when compared with IFN-β binding to IFNAR1-ECD (Table 1). These data suggest that individually Y^{240} and Y^{274} make minor contributions to IFN-β binding and affinity for IFNAR1-ECD, but that together they have a synergistic effect, dramatically influencing the interaction.

Mutations introduced onto IFN-β differentially affect IFNAR1 affinity—Since we had demonstrated the importance of IFNAR1 residues Y^{240} and Y^{274} to this interface, we next investigated the importance of IFN-β residues that bind these tyrosine residues to this interface. We generated variants of IFN-β by substituting alanine residues pairwise at either $F^{63}L^{64}$, $E^{77}T^{78}$, or $V^{81}R^{82}$, the residues predicted to be the central contacts between IFN-β and IFNAR1 residues Y^{240} and Y^{274} (Fig. 2B). We also generated a multi-site variant of IFN-β by substituting alanine residues at the six residues above, generating IFN-β variant F63A/L64A/E77A/T78A/V81A/R82A, herein referred to as IFN-β FLETVR (Fig. 2B). As these residues are predominantly hydrophobic (F, L, T, V) or ionic (E, R), their collective mutation may compromise the high affinity binding of the IFN-β-IFNAR1 interaction. Initially, circular dichroism

(CD) spectroscopy was used to compare the overall fold of IFN-β and its variants and demonstrated that the single- and multi-site alanine substitutions introduced onto IFN-β did not alter the α-helical structure of the proteins (Fig. 2C).

We next used SPR to measure the affinity of IFN-β and its variants to IFNAR1-ECD. Comparison of the measured affinities of IFN-β and the IFN-β variants to immobilized IFNAR1-ECD showed that none of the single site variants IFN-β FL63AA, IFN-β ET77AA or IFN-β VR81AA showed a significant reduction in affinity for IFNAR1 compared to IFN-β (Table 1). By comparison, the multi-site variant IFN-β FLETVR showed a significant ~165-fold reduction in IFNAR1 affinity (Table 1). Overall, these results suggest that, although the mutations introduced at $F^{63}L^{64}$, $E^{77}T^{78}$ and $V^{81}R^{82}$ had insignificant effects on IFNAR1 affinity, the combination of all six residues had the greatest effect on affinity of IFN-β for IFNAR1.

IFNAR1 residues Y^{240} and Y^{274} are important for IFN-β-mediated signaling—To compare the contributions made by residues Y^{240} and Y^{274} to signal transduction by IFN-β, we generated variants of full length IFNAR1 housing tyrosine to alanine mutations at Y^{240} (IFNAR1Y240A), at Y^{274} (IFNAR1Y274A) or at both residues (IFNAR1Y240A/Y274A herein referred to as IFNAR1YYAA) (Fig. 2A). We used transient transfection of *Ifnar1*$^{-/-}$ MEFs to express full-length IFNAR1 or the variants above on the surface of these cells. We confirmed the presence of equivalent levels of IFNAR1 mRNA in the transfected *Ifnar1*$^{-/-}$ MEFs using RT-PCR (Supplemental Fig. S1)). Our data showed that after treatment with IFN-β, cells transfected with all IFNAR1 variant receptors showed a reduced Interferon Stimulated Response Element (ISRE)-luciferase response compared to cells transfected with IFNAR1 (Fig. 3A; *P<0.01*). Cells transfected with either IFNAR1Y240A or IFNAR1Y274A showed relatively minor differences in the luciferase response (showing 20% and 28% reductions, respectively, *P<0.01*), whereas cells transfected with IFNAR1YYAA demonstrated an 85% reduction in luciferase response compared to that measured by IFN-β stimulation through the IFNAR1 receptor (Fig. 3A, *P<0.001*). To investigate IFN subtype specificity of the interface on IFNAR1-SD3 we assessed the use of IFNAR1 receptor variants for signaling by IFNα. Our data show that compared to IFNAR1, transfection of cells with IFNAR1Y240A or IFNAR1YYAA reduced IFNα-driven ISRE-luciferase responses in these cells by 91% and 100%, respectively (Fig. 3B). By contrast, cells transfected with IFNAR1Y274A showed a 33% reduction (relative to IFNAR1) in the IFNα-driven ISRE-luciferase response (Fig. 3B). Comparison of the pattern of IFN-β- and IFN-α-induced ISRE-luciferase responses transduced via IFNAR1Y240A was remarkably different between these IFN subtypes, suggesting that the interface on IFNAR1-SD3, incorporating both Y^{240} and Y^{274}, is used differentially by IFN-β compared to IFN-α.

IFN-β residues binding IFNAR1 Y^{240} and Y^{274} are important for signaling—Having shown that the IFN-β variant proteins retained their native fold and that some demonstrated reduced affinity for IFNAR1-ECD, we next assessed their ability to signal by driving an ISRE-luciferase reporter in a transient transfection system. We transfected *Ifnar1*$^{-/-}$ MEFs with IFNAR1 and stimulated these cells with 2.5 ng/mL of either IFN-β, IFN-β FL63AA, IFN-β ET77AA, IFN-β VR81AA, or IFN-β FLETVR. Our results showed that stimulation of cells with the single-site variants, IFN-β FL63AA, IFN-β ET77AA and IFN-β VR81AA, showed a trend to reduction in the induced luciferase response that was not significantly different from cells stimulated with IFN-β (Fig. 3C). In contrast, cells treated with IFN-β FLETVR induced a consistent and significantly reduced luciferase response (reduced by 45%) compared to cells stimulated with IFN-β (Fig. 3C). Although none of the single-site IFN-β variants showed a significant contribution to the IFN-β-induced ISRE-luciferase response, these data suggest that IFN-β residues $F^{63}L^{64}$, $E^{77}T^{78}$ and $V^{81}R^{82}$ cooperate to synergistically support IFN-β-driven signaling via the critical IFNAR1-SD3 interface.

The IFN-β-IFNAR1-SD3 interface controls down regulation of endogenous IFNAR1—Having shown that the combined substitutions introduced onto IFN-β significantly affected both IFNAR1 binding affinity and signaling, we next measured their effect on the down regulation of IFNAR1 from the surface of cells (11,14). We observed that IFN-β significantly reduced surface levels of IFNAR1 in a dose-dependent manner and at all

doses investigated (Fig. 4A). In comparison, IFN-β FLETVR did not significantly remove IFNAR1 from the surface of cells, even at doses 30 times higher than IFN-β (at 0.3 ng/ml) which did induce significant IFNAR1 downregulation (Fig. 4A). Since IFN-β FLETVR showed a lower binding affinity for IFNAR1 than IFN-β, we assessed whether the lack of observable IFNAR1 down regulation may be due to the short time course of this experiment (1 hour) and carried out an experiment over 48 hours of continuous IFN-β or IFN-β FLETVR stimulation. Again, IFN-β treatment down regulated IFNAR1 from the surface of the cells, and maintained reduced levels of surface IFNAR1 until at least 24 hours after initiation of treatment; by 48 hours of treatment the levels of IFNAR1 on the surface of the cells had returned to levels measurable on untreated cells (Fig. 4B). In comparison, cells treated with IFN-β FLETVR did not show any significant reduction in IFNAR1 surface levels, throughout the 48 hour time-course (Fig. 4B). These data suggest that the residues of IFN-β mutated to generate the IFN-β FLETVR variant are crucial for the IFN-β-driven down-regulation of endogenous IFNAR1 from the cell surface.

The IFN-β-IFNAR1-SD3 interface governs STAT1 activation and gene induction—Since our results had shown that the IFN-β FLETVR variant had a reduced ability to activate the STAT responsive ISRE reporter, we next determined whether IFN-β FLETVR could activate STAT1 via the endogenous IFNAR1 receptor on mouse cells. Our results showed that stimulation of cells with IFN-β induced rapid phosphorylation of STAT1 Y^{701} within 30 minutes of treatment, with no discernible difference between the low (1 ng/ml) and high (5 ng/ml) doses applied (Fig. 5A, B); a significant reduction in IFN-β induced STAT1 phosphorylation was evident after 120 minutes. Following stimulation with IFN-β FLETVR, we observed reduced STAT1 phosphorylation after 30 minutes of treatment compared to cells treated with IFN-β at both doses (1 and 5 ng/mL); STAT1 phosphorylation was barely detectable after 120 minutes (Fig. 5A, B). Overall, our results show that although IFN-β FLETVR could induce some STAT1 phosphorylation, levels were significantly reduced compared to those measured in cells treated with IFN-β (Fig. 5A, B).

We next investigated whether IFN-β FLETVR could induce the expression of ISGs in mouse cells. IFN-β induced the expression of all ISGs investigated (*Ccl2, Cxcl10, Ccl7, Ifit1, Irf1, Bst2, Irf7, Stat1* and *Oas2*) with different dose-dependencies (Fig. 6). In comparison, the magnitude of ISG induction was significantly reduced upon stimulation with IFN-β FLETVR (Fig. 6). We observed that IFN-β FLETVR induced some ISGs (*Ccl2*, *Ccl7*, and *Cxcl10*) at levels not significantly different from those measured in untreated cells, suggesting that efficient induction of these genes is reliant on a high affinity IFN-β-IFNAR1 interaction (Fig. 6). Interestingly, for another subset of genes – *Ifit1, Irf1, Bst2, Irf7, Stat1,* and *Oas2* – we observed induction by IFN-β FLETVR in a dose dependent manner, but significantly less than that observed with IFN-β (Fig. 6). Taken together, these data suggest that the residues mutated to generate IFN-β FLETVR are important for efficient IFN-β-driven STAT1 phosphorylation and gene induction.

The IFN-β-IFNAR1-SD3 interface regulates ligand-dependent biological activities—We next investigated the effect that these mutations and the resultant altered downstream signaling events had on the biological activities elicited by the IFN-β FLETVR variant. We compared the anti-viral and anti-proliferative activities of IFN-β and the IFN-β FLETVR variant. Compared to the specific anti-viral activity of IFN-β, IFN-β FLETVR demonstrated a ~186-fold reduction in its ability to protect mouse cells from infection by Semliki Forest Virus (SFV) (Fig. 7A) suggesting that the IFNAR1-SD3 interface influences the anti-viral properties of IFN-β.

To assess the effect of IFN-β mutations on the anti-proliferative capacity of the protein, we compared the ability of IFN-β and IFN-β FLETVR to inhibit the proliferation of a mouse cell line. In this assay, IFN-β induced ~80% inhibition in cellular proliferation even at the lowest dose applied (Fig. 7B). In comparison, although treatment of cells with IFN-β FLETVR also showed a dose response in inhibition of cellular proliferation (Fig. 7B), the extent of inhibition was significantly reduced compared to that induced by IFN-β (Fig. 7B). These results suggest that the interface on IFNAR1-SD3 also influences the ability of IFN-β to inhibit cellular proliferation.

DISCUSSION

IFN-β plays important roles in activating innate and adaptive immunity, however excessive IFN-β signaling has been implicated in the pathogenesis of several diseases. Detrimental roles for IFN-β and/or its receptor IFNAR1 have been described during sepsis (15-17), bacterial infections including *Listeria* and *Mycobacterium spp.* (18), parasitic infections caused by *Trypanosoma* and *Leishmania spp.* (18), chronic viral infection (8,19) and in the transmission of neuropathic pain (20). It has been hypothesized that a targeted reduction in IFN-β-IFNAR1 signals may be sufficient to protect the host against the lethality of experimental sepsis (21). We previously characterized the importance of IFN-β binding to IFNAR1 in pro-inflammatory responses and here we identified a key interaction interface mediated by two residues on IFNAR1, Y^{240} and Y^{274}, which interact with particular residues on IFN-β (F^{63}, L^{64}, E^{77}, T^{78}, V^{81}, and R^{82}). We demonstrated that this interface stabilizes the ligand-receptor complex, and influences all aspects of IFN-β functionality suggesting that this interface may be a suitable target for rational drug design to therapeutically modulate IFN-β-mediated signaling.

We and others have shown that the minimal ligand binding region for IFNs on IFNAR1 generally exists on the three membrane distal subdomains of this receptor (12). More specifically for IFN-β, we have further shown that the interface spanning both Y^{240} and Y^{274} on IFNAR1-SD3 is most vital to IFNAR1 binding and IFN-β function. Since both these residues made multiple interactions with residues on IFN-β, not just via their hydroxyl groups, we chose to replace both residues with alanine to generate the most unambiguous results. Of these residues, Y^{240} is well conserved across species (Supplementary Fig S2A); our data clearly demonstrate a greater reliance on this residue for efficient IFN-α- compared to IFN-β-mediated signal transduction, an observation that is supported in the literature (10). The second tyrosine residue we identified in the interface on IFNAR1-SD3, Y^{274}, is not conserved across species (Supplementary Fig S2A); indeed the residue to which it aligns in human IFNAR1 (Q^{272}) was not identified as important in the IFN-ω-IFNAR1 interface (10). Our data, however, suggests that IFN-β and IFN-α both partially utilize this residue on mouse IFNAR1 for an efficient ISRE-dependent response. That IFN-β seems to utilize this residue in synergy with Y^{240} for efficient signal transduction suggests that the interface spanning these two residues may be a site of species or IFN subtype specificity.

From the ligand perspective, residues we identified as important in the mouse IFN-β-IFNAR1-SD3 interface are variably conserved across species and/or IFN subtype (Supplementary Fig S2B). F^{63}, E^{77} and T^{78} are highly conserved across IFN subtype and species; whilst the homolog to F^{63} in human IFN-ω (F^{67}) is important in the IFN-ω-IFNAR1 interface, the residues to which E^{77} and T^{78} align (M^{81} and T^{82}, respectively) were not identified as important to the IFN-ω-IFNAR1 interaction, supporting the potential involvement of this site in the ligand discrimination mechanism exhibited by IFNAR1 (10). Indeed, E^{77}, T^{78} and R^{82} in the IFN-β-IFNAR1-SD3 interface bind exclusively to Y^{274} of IFNAR1 (11), further supporting the unique dependence on this tyrosine residue for IFN-β-mediated signaling. While the presence of a valine at position 81 (V^{81}) seems to be unique to mouse IFN-β, the residue to which V^{81} structurally aligns in human IFN-ω (D^{85}) has been shown to be involved in the hIFNAR1 interface (10). Disparity in the reduction in signals transduced by IFNAR1 residues versus IFN-β residues (F^{63}, L^{64}, E^{77}, T^{78}, V^{81}, and R^{82}) in the IFN-β-IFNAR1-SD3 interface suggests that other residues on IFN-β may also contribute to signaling.

Other studies have reported that IFNs with a comparatively lower binding affinity for IFNAR1 show reductions in the ability to down-regulate cell-surface IFNAR1 (22,23), to activate STAT1 and to exert an anti-proliferative response on cells (23). Our findings are consistent with these observations in that targeted abrogation of the high affinity IFN-β-IFNAR1 complex completely abolished down-regulation of endogenous IFNAR1 and activation of these IFN-β-mediated signaling outcomes. From the ligand perspective, our data showed a correlative effect between IFN-β-IFNAR1 binding affinity and the significance of the IFN-β-driven STAT response. These data demonstrate the cumulative effect of IFN-β residues F^{63}, L^{64}, E^{77}, T^{78}, V^{81}, and R^{82} to these biological outcomes of the IFN-β-IFNAR1 interaction. Since we showed that this interface influenced the magnitude of the STAT1-

phosphorylation dependent signaling which has been shown to be vital for protection of cells against viral infection, our findings are also consistent with a role for the identified interface in the anti-viral activity of IFN-β (24). The IFNAR1 and IFNAR2 binding interfaces on the type I IFNS are located on opposing sides of the ligands and seem somewhat independent of each other (10). So although the residues we targeted in this study were found exclusively within the IFN-β-IFNAR1-SD3 interface we do not expect the mutations made to IFN-β to have effected its interaction with IFNAR2. However, this remains to be experimentally determined.

Since we had shown that the IFN-β-IFNAR1-SD3 interface influenced the magnitude of STAT1 activation, for investigation of its effect on gene induction we targeted ISGs that had been reported to be inducible via phospho-STAT1 independent pathways, such as the un-phosphorylated STAT1 pathway (24). Analysis of the genes induced by IFN-β in our study revealed that there was one subset of genes (*Ccl2*, *Cxcl10*, *Ccl7*, *Ifit1*, and *Irf1*) reliant on the high affinity IFN-β-IFNAR1 interaction for efficient gene induction, an observation supported by the literature (23,25-27). Interestingly, the subset of genes previously identified as inducible via an IFN-β-dependent, un-phosphorylated STAT1 mediated anti-viral pathway (*Bst2*, *Irf7*, *Stat1*, and *Oas2*) were less effected by the mutations made to the IFN-β-IFNAR1-SD3 interface (24). Our results therefore suggest that this pathway may be only partially dependent on the high-affinity IFN-β-IFNAR1-SD3 interface identified. We found that mutations made to this interface impacted not only ISG induction but also the ability of IFN-β to inhibit cellular proliferation, as evident from the reduced dose-response curve of the IFN-β-IFNAR1 variant. Mechanistically, these results may therefore point to a role for the identified IFN-β-IFNAR1-SD3 interface in differentially regulating or mediating alternative IFN-β-IFNAR1-driven signaling events or pathways. Our data, demonstrating the functional importance of residues at the IFN-β-IFNAR1-SD3 interface are in contrast to alanine mutations introduced to the (juxta) transmembrane region which predictably had no effect on IFN binding affinity or signaling (28).

Overall, we have characterized and identified an important binding interface between IFN-β and IFNAR1 that is critical for eliciting the full biological response resulting from IFN-β engagement of IFNAR1 – from initial binding to the receptor, to receptor internalization, transcription factor activation, gene induction and biological processes. Importantly, we demonstrated that by modulating this interface we can distinctly alter the biological effects of IFN-β. Thus, in identifying an IFN-β-specific interface on IFNAR1 and elucidating its importance in modulating IFN-β-mediated responses, we provide further insight into how this cytokine functions and reveal an important target for drug discovery to fine-tune IFN-β-driven responses and perhaps mediate subsequent disease.

EXPERIMENTAL PROCEDURES

Cell lines and Cell Culture—Mouse L929 fibroblast cell line was purchased from the American Type Culture Collection and maintained in RPMI 1640 medium supplemented with 10% (v/v) fetal calf serum (Gibco), 50U/mL penicillin, 50U/mL streptomycin (Gibco) at 37ºC, 5% (v/v) CO_2. Mouse embryonic fibroblasts (MEFs) were derived from *Ifnar1*$^{-/-}$ mice as previously published (29) and maintained in Dulbecco's Modified Eagle Medium (DMEM) containing 10% (v/v) fetal calf serum (Gibco), 50U/mL penicillin, 50U/mL streptomycin (Gibco) at 37ºC, 5% (v/v) CO_2. Serum-free adapted insect cell lines Sf9 and High Five™ (BTI-TN-5B1-4 from *Trichoplusia ni)* were purchased from Life Technologies and maintained in Sf900-II SFM media (Life Technologies) supplemented with 1 µg/mL Gentamicin (Sigma-Aldrich) in a shaking incubator at 27°C, 120 rpm. For expression cultures, High Five™ cells were diluted in serum-free Express Five media (Life Technologies) supplemented with 20mM L-Glutamine (Sigma) and 1 µg/mL Gentamicin (Sigma) and incubated at 27°C, 120 rpm.

Constructs and cloning—The clone of mIFNAR1-ECD was as previously reported (11). Constructs encoding truncation variants of IFNAR1-ECD were generated using this clone and the QuikChange mutagenesis kit (Stratagene) to introduce stop codons at the junctions between IFNAR1-ECD subdomains as directed by specific primer pairs (Table 2). Site-directed mutagenesis

was also carried out to introduce alanine mutations at amino acid positions Y^{240} and Y^{274} of this IFNAR1-ECD clone (Table 2). The mIFN-β clone was as previously reported (30). Site-directed mutagenesis was carried out using the QuikChange mutagenesis kit (Stratagene) to introduce pair-wise alanine mutations at amino acid positions F^{63}/L^{64}, E^{77}/T^{78}, and V^{81}/R^{82} of this IFN-β clone as required (Table 2).

Recombinant protein expression, purification and Native PAGE—All recombinant IFNAR1-ECD and IFN-β forms were expressed using a baculoviral expression system and purified as previously published (11,30). The mIFN-α1 utilized in this project was expressed by transient transfection in HEK293S cells and purified from culture supernatants as previously described (31). The purity of all protein preparations was checked on reducing SDS-PAGE prior to use in experiments. All interactions and Native PAGE were carried out as previously published (11) using 8% polyacrylamide gels.

CD Spectroscopy—CD spectral analyses were measured at room temperature in a Jasco J815 CD spectrophotometer. All scans were run on proteins concentrated to 130µg/mL in TBS (10mM Tris, pH 8.0, 150 mM sodium chloride). Triplicate scans were run between 190 and 260 nm. Data were collected and converted to mean residue ellipticity (MRE) by the equation of Correa and Ramos (32). Data is representative of triplicate experiments.

SPR —All SPR experiments were carried out on a ProteOn XPR36 (Bio-rad Labs) using a HTG chip for His-tagged proteins and TBS as the running buffer. All ligands (IFNAR1-ECD and variants) were immobilized to the nickel activated chip via the His-tags after dilution to 25 µg/mL in TBS (10mM tris, pH 8.0, 150 mM sodium chloride). All analyte samples (IFN-β and variants) were diluted in TBS to various concentrations ranging from 40 nM to 1 uM. All data were referenced according to the manufacturer's instructions (Bio-Rad) and analyzed using the Langmuir binding model. Data were considered for inclusion in the analysis only if the Chi^2 value (the measure of error between measured and fitted values) was less than 10% of the R_{max} as per the manufacturer's instructions (Bio-Rad). k_a (1/Ms), k_d (1/s), and K_D (nM) were calculated by the Proteon Manager software and are represented as mean from at least triplicate experiments. Significance was determined using one-way ANOVA with Dunnett's multiple comparisons testing.

Transient transfections of Ifnar1$^{-/-}$ MEFs and luciferase assays—Ifnar1$^{-/-}$ MEFs were used for all transient transfections of IFNAR1 or its variants as previously reported (33). Cells were incubated at 37ºC, 5% (v/v) CO_2 for ~20 hours prior to the addition of any stimuli. To test for comparative expression of introduced *Ifnar1* mRNA, cells were harvested after the 20 hours incubation without any stimulation. For luciferase assays, we co-transfected an ISRE-luciferase reporter (as previously published in (33)) as a measure of STAT activation induced by IFN stimulations. All stimulations were carried out with continuous IFN treatment (2.5 ng/mL of culture), with cells harvested for luciferase assays after 4 hours incubation at 37ºC, 5% (v/v) CO_2. After incubation, cells were lysed in passive lysis buffer (Promega); luciferase and TK-Renilla activity were assessed as previously described (33). All transfections were carried out in at least biological and technical triplicate for each sample with readings normalized to that of TK-Renilla. Results are presented as luminescence measurable per treatment above those measured in cells transfected with vector alone, and then converted to percentage of the luciferase response measured on cells transfected with IFNAR1 and treated with IFN. Significance of responses were calculated using a 2-way ANOVA with Tukey's multiple comparisons testing.

Cell lysis, SDS-PAGE and Western blot—We used L929 cells stimulated with IFN-β or the IFN-β FLETVR variant to compare the ability of these proteins to induce phosphorylation of STAT1 (at Y^{701}). Cells were plated at 6 x 10^5 cells per well of a 6 well cell culture dish and incubated overnight at 37ºC, 5% (v/v) CO_2. After the end-point of stimulation, media was aspirated, cells rinsed with PBS and lysed in cell lysis buffer as previously reported (11). Protein concentrations in cell lysates were quantified using Lowry reagents (Bio-rad) and assayed using a FLUOstar Optima microplate reader (BMG Technologies). Seven to 15 µg of whole cell lysate was separated on a 10% (v/v) SDS-PAGE (34) and transferred to PVDF membrane (Immobilon FL, Millipore) using a Mini Trans-Blot apparatus (Bio-rad). Membranes were blocked in Odyssey blocking buffer (OBB;

Millenium Sciences) for 1 hour at 22ºC. Membranes were incubated with primary antibodies (anti-phospho-Y701 STAT1 (Cat No 7649S, clone D4A7; 1:1000, Cell Signaling Technologies), total anti-mouse STAT1 (Cat No sc-346, clone E-23; 1:200, Santa Cruz Biotechnologies) or anti-actin antibodies (Cat No A4700, clone AC-40; 1:500, Sigma)) diluted in fresh OBB for 16 hours at 4ºC. Binding of secondary antibodies (AlexaFluor 680-conjugated anti-mouse IgG (1:1000, Cat No A21057, Life Technologies); IR800-conjugated anti-rabbit IgG (1:1000, Cat No 611-145-002-0 5, Rockland)) diluted in OBB was carried out for 1 hour at 22ºC. Antibody binding was detected using an Odyssey Infra-Red Imager (Li-Cor). Densitometry of the detected bands was quantitated using ImageJ; the levels of detectable phospho-STAT1 were normalized to the level of actin for each sample (triplicate experiments). The blots shown are representative of triplicate independent experiments. Significance of responses were calculated using a 2-way ANOVA with Tukey's multiple comparisons testing.

Extraction of RNA and cDNA synthesis for quantitative Real-Time PCR—To evaluate gene expression by quantitative real-time PCR (RT-PCR), L929 cells were plated at 6 x 10^5 cells per well of a 6 well cell culture dish and incubated overnight at 37ºC, 5% (v/v) CO_2. After 3 hours of treatment, cells were lysed in RLT buffer and RNA purified using the RNeasy column purification kit (Qiagen); all cDNA synthesis was prepared using Superscript III First Strand cDNA kit (Invitrogen) and random hexamers (Invitrogen) following the manufacturer's protocol. Quantitative RT-PCR was performed on an Applied Biosystems 7900HT Fast Real-Time PCR system (ABI) using Sybr reagents (ABI); amplification was directed by the forward and reverse primer pairs indicated (Table 2). All experiments were carried out with biological and technical triplicates (except where stated) with data normalized relative to the expression of 18S and transformed using the $\Delta\Delta C_T$ method (35). Data are presented as fold induction relative to unstimulated control samples and reported as mean $\pm$ SD of at least triplicate independent experiments. Significant difference in fold induction between untreated, IFN-β and IFN-β FLETVR treated samples was calculated using 2-way ANOVA with either Sidak's multiple comparisons testing (to compare mRNA levels measured in IFN-β and IFN-β FLETVR treated samples) or Dunnett's multiple comparisons testing (to compare mRNA levels measured in all stimulated cells with that in untreated cells).

Flow cytometry—Flow cytometry was used to measure and compare the effect of stimulation with IFN-β or the IFN-β FLETVR variant on surface levels of IFNAR1 on L929 cells. The anti-mouse IFNAR1 antibody (Cat No I-401, Clone Mar1-5A3, Leinco) was as reported in (36) and its isotype counterpart (Cat Nos I536, Clone HKSP84, Leinco) were biotinylated using EZ™-Link NHS-Biotin following the manufacturers' instructions (Thermo Scientific). For flow cytometry, L929 cells were plated at 2 x 10^5 cells/well of a 24 well culture plate and incubated at 37ºC, 5% (v/v) CO_2 overnight. After stimulation, cells were harvested from the culture vessel using cell suspension buffer (PBS with 2% (v/v) fetal calf serum) containing 5mM EDTA, and then centrifuged at 1500 rpm for 5 minutes. Non-specific antibody interactions were blocked using anti-CD16/CD32 blocking antibody (Cat No 14-0161-86, clone p3; eBiosciences diluted 1:200) prior to staining with either biotinylated anti-mouse IFNAR1 or the biotinylated isotype control antibody both diluted to 10 µg/mL in cell suspension buffer. Antibody binding was detected using a Phycoerythrin (PE)-conjugated Streptavidin secondary antibody (Cat No F0040, R&D systems diluted 1:1000). All cell staining was analyzed on a FACSCanto II (Becton Dickinson). Data are given as mean fluorescence intensity (MFI) of anti-mouse IFNAR1 staining above levels of isotype control antibody staining, and are reported as mean of at least triplicate independent biological replicates. Significance of responses were calculated using a one-way ANOVA with Dunnett's multiple comparisons testing.

Anti-viral activity of IFN—Antiviral activities of IFN-β and the IFN-β FLETVR variant were determined by cytopathic effect inhibition assay using mouse L929 cells and SFV for infection (37). Activity was measured against a National Institutes of Health reference standard (GU-02-901-511) as published previously (37) and is reported as the concentration of IFN that is required to provide protection to 50% of the exposed cells (ED_{50}). Data are given as specific activity (IU/mg of protein), and are reported as the

average from at least triplicate independent experiments. Student's *t*-test was applied to the two groups to determine significance.

Measurement of anti-proliferative activity—For assessment of the ability of IFN-β and its variants to inhibit cellular proliferation, 6 x 10^4 L929 cells were plated per well of a 96 well E-plate (Roche Diagnostics) and monitored using the xCELLigence Real-Time Cell Analyzer SP Instrument (Roche Diagnostics) at 37°C in 5% (v/v) CO_2. Cell index (CI) measurements were performed in quadruplicate per stimulation and signal was detected every 30 minutes. For analysis, the CI index was normalised to time of treatment and the slope (1/h) was calculated from normalised CI to 72h post treatment using the Real-Time Cell Analyzer software (Version 1.2, Roche Diagnostics). All treatment analysis was compared to the slope of buffer control treated cells. Data is expressed as mean ± SD of triplicate independent experiments, performed in technical quadruplicate, and analyzed using 2-way ANOVA with Sidak's multiple comparisons test.

Acknowledgements: Funding sources: NDW is supported by NHMRC New Investigator grant (2014-2016, APP1070732) and an NHMRC project grant (APP1126524). JV is supported by an NHMRC project grant (APP1126524). JR is supported by an ARC Laureate Fellowship. PJH is supported by an NHMRC SPRF Fellowship (APP1117527) and NHMRC project grant (APP1126524).

Conflict of interest: The authors declare that they have no conflicts of interest with the contents of this article.

Author contributions: NDW conceived the idea for the project, conducted most of the experiments, analyzed the data, and wrote the manuscript. AYM carried out mutagenesis, prepared recombinant proteins, conducted experiments in anti-viral assays. PRP carried out luciferase assays, gene expression assays and data analysis. NMB carried out anti-proliferative assays, data analysis and helped prepare the manuscript. SSL carried out Western blots and data analysis. JPV helped conceive concepts for the project, carried out structure analysis, and helped prepare the manuscript. JR contributed to experimental planning, structure analysis and helped prepare the manuscript. PJH contributed to experimental planning and contributed to preparation of the manuscript.

REFERENCES

1. Pestka, S. (2007) The interferons: 50 years after their discovery, there is much more to learn. *J Biol Chem* **282**, 20047-20051
2. Medzhitov, R. (2001) Toll-like receptors and innate immunity. *Nat Rev Immunol* **1**, 135-145
3. Jonasch, E., and Haluska, F. G. (2001) Interferon in oncological practice: review of interferon biology, clinical applications, and toxicities. *Oncologist* **6**, 34-55
4. Annibali, V., Mechelli, R., Romano, S., Buscarinu, M. C., Fornasiero, A., Umeton, R., Ricigliano, V. A., Orzi, F., Coccia, E. M., Salvetti, M., and Ristori, G. (2015) IFN-beta and multiple sclerosis: from etiology to therapy and back. *Cytokine Growth Factor Rev* **26**, 221-228
5. Lebrun, C., Bertagna, M., and Cohen, M. (2011) Cutaneous Side-effects of Immunomodulators in MS. *Int MS J* **17**, 88-94
6. Platanias, L. C. (2005) Mechanisms of type-I- and type-II-interferon-mediated signalling. *Nat Rev Immunol* **5**, 375-386
7. Coelho, L. F., Magno de Freitas Almeida, G., Mennechet, F. J., Blangy, A., and Uze, G. (2005) Interferon-alpha and -beta differentially regulate osteoclastogenesis: role of differential induction of chemokine CXCL11 expression. *Proc Natl Acad Sci U S A* **102**, 11917-11922
8. Ng, C. T., Sullivan, B. M., Teijaro, J. R., Lee, A. M., Welch, M., Rice, S., Sheehan, K. C., Schreiber, R. D., and Oldstone, M. B. (2015) Blockade of interferon Beta, but not interferon alpha, signaling controls persistent viral infection. *Cell host & microbe* **17**, 653-661
9. Deonarain, R., Verma, A., Porter, A. C., Gewert, D. R., Platanias, L. C., and Fish, E. N. (2003) Critical roles for IFN-beta in lymphoid development, myelopoiesis, and tumor development: links to tumor necrosis factor alpha. *Proc Natl Acad Sci U S A* **100**, 13453-13458
10. Thomas, C., Moraga, I., Levin, D., Krutzik, P. O., Podoplelova, Y., Trejo, A., Lee, C., Yarden, G., Vleck, S. E., Glenn, J. S., Nolan, G. P., Piehler, J., Schreiber, G., and Garcia, K. C. (2011) Structural Linkage between Ligand Discrimination and Receptor Activation by Type I Interferons. *Cell* **146**, 621-632
11. de Weerd, N. A., Vivian, J. P., Nguyen, T. K., Mangan, N. E., Gould, J. A., Braniff, S. J., Zaker-Tabrizi, L., Fung, K. Y., Forster, S. C., Beddoe, T., Reid, H. H., Rossjohn, J., and Hertzog, P. J. (2013) Structural basis of a unique interferon-beta signaling axis mediated via the receptor IFNAR1. *Nat Immunol* **14**, 901-907
12. Lamken, P., Gavutis, M., Peters, I., Van der Heyden, J., Uze, G., and Piehler, J. (2005) Functional cartography of the ectodomain of the type I interferon receptor subunit ifnar1. *J Mol Biol* **350**, 476-488
13. Lee, B., and Richards, F. M. (1971) The interpretation of protein structures: estimation of static accessibility. *J Mol Biol* **55**, 379-400
14. Marijanovic, Z., Ragimbeau, J., van der Heyden, J., Uze, G., and Pellegrini, S. (2007) Comparable potency of IFNalpha2 and IFNbeta on immediate JAK/STAT activation but differential down-regulation of IFNAR2. *Biochem J* **407**, 141-151
15. Karaghiosoff, M., Steinborn, R., Kovarik, P., Kriegshauser, G., Baccarini, M., Donabauer, B., Reichart, U., Kolbe, T., Bogdan, C., Leanderson, T., Levy, D., Decker, T., and Muller, M. (2003) Central role for type I interferons and Tyk2 in lipopolysaccharide-induced endotoxin shock. *Nat Immunol* **4**, 471-477
16. Mahieu, T., Park, J. M., Revets, H., Pasche, B., Lengeling, A., Staelens, J., Wullaert, A., Vanlaere, I., Hochepied, T., van Roy, F., Karin, M., and Libert, C. (2006) The wild-derived inbred mouse strain SPRET/Ei is resistant to LPS and defective in IFN-beta production. *Proc Natl Acad Sci U S A* **103**, 2292-2297

17. Dejager, L., Vandevyver, S., Ballegeer, M., Van Wonterghem, E., An, L. L., Riggs, J., Kolbeck, R., and Libert, C. (2014) Pharmacological inhibition of type I interferon signaling protects mice against lethal sepsis. *J Infect Dis* **209**, 960-970
18. Stifter, S. A., and Feng, C. G. (2015) Interfering with immunity: detrimental role of type I IFNs during infection. *J Immunol* **194**, 2455-2465
19. Wilson, E. B., Yamada, D. H., Elsaesser, H., Herskovitz, J., Deng, J., Cheng, G., Aronow, B. J., Karp, C. L., and Brooks, D. G. (2013) Blockade of chronic type I interferon signaling to control persistent LCMV infection. *Science* **340**, 202-207
20. Stokes, J. A., Cheung, J., Eddinger, K., Corr, M., and Yaksh, T. L. (2013) Toll-like receptor signaling adapter proteins govern spread of neuropathic pain and recovery following nerve injury in male mice. *Journal of neuroinflammation* **10**, 148
21. Mahieu, T., and Libert, C. (2007) Should we inhibit type I interferons in sepsis? *Infect Immun* **75**, 22-29
22. Jaitin, D. A., and Schreiber, G. (2007) Upregulation of a small subset of genes drives type I interferon-induced antiviral memory. *J Interferon Cytokine Res* **27**, 653-664
23. Levin, D., Schneider, W. M., Hoffmann, H. H., Yarden, G., Busetto, A. G., Manor, O., Sharma, N., Rice, C. M., and Schreiber, G. (2014) Multifaceted activities of type I interferon are revealed by a receptor antagonist. *Science signaling* **7**, ra50
24. Cheon, H., Holvey-Bates, E. G., Schoggins, J. W., Forster, S., Hertzog, P., Imanaka, N., Rice, C. M., Jackson, M. W., Junk, D. J., and Stark, G. R. (2013) IFNbeta-dependent increases in STAT1, STAT2, and IRF9 mediate resistance to viruses and DNA damage. *EMBO J* **32**, 2751-2763
25. Lehmann, M. H., Torres-Dominguez, L. E., Price, P. J., Brandmuller, C., Kirschning, C. J., and Sutter, G. (2016) CCL2 expression is mediated by type I IFN receptor and recruits NK and T cells to the lung during MVA infection. *J Leukoc Biol*
26. Khorooshi, R., and Owens, T. (2010) Injury-induced type I IFN signaling regulates inflammatory responses in the central nervous system. *J Immunol* **185**, 1258-1264
27. Lin, S. J., Lo, M., Kuo, R. L., Shih, S. R., Ojcius, D. M., Lu, J., Lee, C. K., Chen, H. C., Lin, M., Leu, C. M., Lin, C. N., and Tsai, C. H. (2014) The pathological effects of CCR2+ inflammatory monocytes are amplified by an IFNAR1-triggered chemokine feedback loop in highly pathogenic influenza infection. *Journal of biomedical science* **21**, 99
28. Sharma, N., Longjam, G., and Schreiber, G. (2016) Type I Interferon Signaling Is Decoupled from Specific Receptor Orientation through Lenient Requirements of the Transmembrane Domain. *J Biol Chem* **291**, 3371-3384
29. Zhao, W., Lee, C., Piganis, R., Plumlee, C., de Weerd, N., Hertzog, P. J., and Schindler, C. (2008) A conserved IFN-alpha receptor tyrosine motif directs the biological response to type I IFNs. *J Immunol* **180**, 5483-5489
30. Stifter, S. A., Gould, J. A., Mangan, N. E., Reid, H. H., Rossjohn, J., Hertzog, P. J., and de Weerd, N. A. (2014) Purification and biological characterization of soluble, recombinant mouse IFNbeta expressed in insect cells. *Protein Expr Purif* **94**, 7-14
31. Bidwell, B. N., Slaney, C. Y., Withana, N. P., Forster, S., Cao, Y., Loi, S., Andrews, D., Mikeska, T., Mangan, N. E., Samarajiwa, S. A., de Weerd, N. A., Gould, J., Argani, P., Moller, A., Smyth, M. J., Anderson, R. L., Hertzog, P. J., and Parker, B. S. (2012) Silencing of Irf7 pathways in breast cancer cells promotes bone metastasis through immune escape. *Nat Med* **18**, 1224-1231
32. Correa, D. H. A., and Ramos, C. H. I. (2009) The use of circular dichroism spectroscopy to study protein folding, form and function. . *African J Biochem Res* **3**, 164-173.
33. Piganis, R. A., De Weerd, N. A., Gould, J. A., Schindler, C. W., Mansell, A., Nicholson, S. E., and Hertzog, P. J. (2011) Suppressor of cytokine signaling (SOCS) 1 inhibits type I interferon (IFN)

signaling via the interferon alpha receptor (IFNAR1)-associated tyrosine kinase Tyk2. *J Biol Chem* **286**, 33811-33818
34. Laemmli, U. K. (1970) Cleavage of structural proteins during the assembly of the head of bacteriophage T4. *Nature* **227**, 680-685
35. Yuan, J. S., Reed, A., Chen, F., and Stewart, C. N., Jr. (2006) Statistical analysis of real-time PCR data. *BMC Bioinformatics* **7**, 85-96
36. Sheehan, K. C., Lai, K. S., Dunn, G. P., Bruce, A. T., Diamond, M. S., Heutel, J. D., Dungo-Arthur, C., Carrero, J. A., White, J. M., Hertzog, P. J., and Schreiber, R. D. (2006) Blocking monoclonal antibodies specific for mouse IFN-alpha/beta receptor subunit 1 (IFNAR-1) from mice immunized by in vivo hydrodynamic transfection. *J Interferon Cytokine Res* **26**, 804-819
37. Hwang, S. Y., Hertzog, P. J., Holland, K. A., Sumarsono, S. H., Tymms, M. J., Hamilton, J. A., Whitty, G., Bertoncello, I., and Kola, I. (1995) A null mutation in the gene encoding a type I interferon receptor component eliminates antiproliferative and antiviral responses to interferons alpha and beta and alters macrophage responses. *Proc Natl Acad Sci U S A* **92**, 11284-11288

FOOTNOTES: The abbreviations used are: IFNAR, IFN-α/β receptor; SD, subdomain; STAT, Signal transducer and Activator of Transcription; ECD, extracellular domain; ISGs, interferon stimulated genes; N-terminal, amino-terminal; C-terminal, carboxyl-terminal; SPR, Surface Plasmon Resonance; CD, Circular Dichroism; MEFs mouse embryonic fibroblasts; ISRE, interferon stimulated response element; PE phycoerythrin; SFV, Semliki Forest Virus; DMEM, Dulbecco's Modified Eagle Medium; TBS, tris-buffered saline; MRE mean residue ellipticity; RT-PCR, quantitative real-time PCR; MFI, mean fluorescence intensity; ANOVA, Analysis of variance; CI, cell index; OBB Odyssey blocking buffer.

Table 1. Surface Plasmon Resonance (SPR) measurements of IFN-β and mutants binding to IFNAR1 and the mutant receptors as indicated. Association (k_a), Dissociation (kd) and Affinity (KD) are indicated. Data are represented as mean ± SEM of a least triplicate independent experiments. Significance of comparisons calculated relative to the KD of the IFNAR1-IFN-β interaction. **** P < 0.0001 (1-way ANOVA with Dunnett's multiple comparisons testing).

Receptor	**IFN**	**k_a (1/Ms) (Mean)**	**k_d (1/s) (Mean)**	**K_D (nM) (Mean ± SD)**	**Fold increase (K_D) compared to IFNβ**	**Significance (K_D) from IFNβ**
IFNAR1-ECD	IFN-β	1.55×10^5	3.77×10^{-4}	3.34 (± 2.23)	1	-
IFNAR1-ECDY240A	IFN-β	4.66×10^5	1.16×10^{-2}	29.1 (± 15.5)	8.71	NS
IFNAR1-ECDY274A	IFN-β	5.39×10^4	8.58×10^{-4}	20.6 (± 12)	6.17	NS
IFNAR1-ECDYYAA	IFN-β	4.07×10^5	9.79×10^{-2}	232 (± 67.2)	69.46	****
IFNAR1-ECD	IFN-β FL63AA	7.40×10^5	7.85×10^{-3}	16.8 (± 5.65)	3.00	NS
IFNAR1-ECD	IFN-β ET77AA	8.87×10^4	8.51×10^{-4}	12.1 (± 5.8)	3.62	NS
IFNAR1-ECD	IFN-β VR81AA	5.27×10^5	1.76×10^{-3}	7.44 (± 3.72)	2.22	NS
IFNAR1-ECD	IFN-β FLETVR	9.86×10^4	4.65×10^{-2}	552 (± 175)	165.27	****

Table 2. Primers utilised in this study, and the purpose for which they were used.

Primer name or purpose	**Primer Sequence 5' to 3' Forward**	**Primer Sequence 5' to 3' Reverse**
MUTAGENESIS		
Introduce stop codon at V205 in IFNAR1	NA	CTTGGAGATTTCCTGGTCAAGGCATTTTATTTGC
Introduce stop codon at P309 in IFNAR1	NA	GTTAAGCTTAAGGAGGGAGAATGTGTTT
IFNAR1 Y240 to A	GTGGCTTCCTGGCGCTTCAAAAAGCAG	CTGCTTTTTGAAGCGCCAGGAAGCCAC
IFNAR1Y274 to A	CTCAAGATACTGTCGCCACAGGAACGTTCTTTCTC	GAGAAAGAACGTTCCTGTGGCGACAGTATCTTGAG
IFN-β F63/L64 to AA to IFN-β FL63AA	GAGTGCTCCAGAATGTCGCTGCTGTCTTCAGAAACAATTTC	GAAATTGTTTCTGAAGACAGCAGCGACATTCTGGAGCATCTC
IFN-β E77/T78 to AA to IFN-β ET77AA	CTCCAGCACTGGGTGGAATGCGGCTATTGTTGTACGTCTCCTG	CAGGAGACGTACAACAATAGCCGCATTCCACCCAGTGCTGGAG
IFN-β V81/R82 to AA to IFN-β VR81AA	GGAATGAGACTATTGTTGCAGCTCTCCTGGATGAACTCCAG	GTGGAGTTCATCCAGGAGAGCTGCAACAATAGTCTCATTCC
IFN-β to ET77AA on IFN-β V81/R82aa backbone to generate FLETVR	CTCCAGCACTGGGTGGAATGCGGCTATTGTTGCAGCTCTCCTG	CAGGAGAGCTGCAACAATAGCCGCATTCCACCCAGTGCTGGAG
RT-PCR		
m18S	GTAACCCGTTGAACCCCATT	CCATCCAATCGGTAGTAGCG
mOas1a	CCTGCACAGACAGCTCAGAA	AGCCACACATCAGCCTCTTC
mISG15	TGAGAGCAAGCAGCCAGAAG	ACGGACACCAGGAAATCGTT
mIRF7	ATCTTGCGCCAAGACAATTC	AGCATTGCTGAGGCTCACTT
mBst2	GGAGTCCCTGGAGAAGAAGG	GGAGTCCCTGGAGAAGAAGG
mCCL2	AGGTGTCCCAAAGAAGCTGTA	ATGTCTGGACCCATTCCTTCT
mCCL7	AGATCCCCAAGAGGAATCTCA	ATAGCCTCCTCGACCCACTT
mCXCL10	CTGAATCCGGAATCTCCGACC	GAGGCTCTCTGCTGTCCATC

mIfit1	TCAAGGCAGGTTTCTGAGGA	ACCTGGTCACCATCAGCATT
mIrf1	AGCTGCAAAGAGGAACCAGA	CTCACAGAGTTGCCCAGCAG
mStat1	TCACATTCACATGGGTGGAA	CGGCAGCCATGACTTTGTAG
mIfnar1-Neo	GTGGGCACTGGAGAAACCT	TGACGGATGTATTGCTTTAACTTCT
mIfnar1	GCAGTGTGACCTTTTCAGCA	GAGAATTCACACTTGGTCGTTG

FIGURE LEGENDS

FIGURE 1. Contributions of IFNAR1 subdomains (SD) 1-4 to IFN-β binding. (A) The crystal structure of IFNAR1 (blue) in complex with IFN-β (yellow). Relative percentage contributions of each domain of IFNAR1 to the overall IFN-β binding interface (crystal structure of the IFN-β-IFNAR1 complex from (11); PDB code 3WCY). (B) The helices of IFN-β (A to E) and the IFNAR1 subdomains (SD1-4) are indicated. The positions of Y^{240} and Y^{274} are indicated with dark blue spheres. (C) Close-up view of the binding of Y^{240} and Y^{274} (blue sticks) to residues on the B and C helices of IFN-β (yellow sticks). (D) Diagrammatic representation of IFNAR1-ECD truncation variants generated in this study. (E) Native PAGE (10% v/v) analysis of IFNAR1-ECD, IFNAR1-SD123, IFNAR1-SD12 alone and with IFN-β. These interactions were carried out in triplicate.

FIGURE 2. IFNAR1 and IFN-β variants generated and assessed in this study. (A) Residues of IFNAR1 were mutated to alanine residues as indicated. IFNAR1 residues 230 to 280 only are shown. (B) Residues of IFNβ were mutated to alanine residues as indicated. IFN-β residues 60 to 90 only are shown. (C) Circular Dichroism analysis confirmed the α-helical fold of IFN-β variants: IFNβ (▬), IFNβ FL63AA (▬), IFNβ ET77AA (.....), IFNβ VR81AA (▬) and IFNβ FLETVR (▬ ▬).

FIGURE 3. IFN specificity and signalling via IFNAR1-ECD SD3 residues. (A, B) Measurement of luciferase activity in cells transfected with vector only (VO), IFNAR1, or the IFNAR1 variant receptors, IFNAR1Y240A, IFNAR1Y274A, IFNAR1YYAA after stimulation with 2.5ng/mL of either IFN-β (A) or mIFNα1 (B) for 4 hours. (C) Measurement of luciferase activity in cells transfected with IFNAR1 after stimulation with 2.5ng/mL of IFN-β or variants, IFN-β FL63AA, IFN-β ET77AA, IFN-β VR81AA, IFN-β FLETVR. Data expressed as mean of at least triplicate independent experiments, all performed with technical triplicate. Significance of response calculated relative to cells transfected with either IFNAR1 constructs (A, B) or treated with IFN-β (C). * $P < 0.05$, ** $P < 0.01$, **** $P < 0.0001$ (2-way ANOVA with Tukey's multiple comparisons testing). Significance of response calculated relative to cells transfected with empty vector only # $P < 0.05$, ## $P < 0.01$ (2-way ANOVA with Tukey's multiple comparisons testing).

FIGURE 4. Abundance of surface levels of IFNAR1 on L929 cells treated with either IFN-β or the IFN-β FLETVR variant (indicated), as measured by flow cytometry. (A) Cells were treated with increasing doses of protein (0.3, 1.0, 2.5, 5.0 and 10 ng/ml) as indicated for 1 hour prior to harvesting and staining. (B) Cells were treated with 1 ng/ml of the proteins indicated and harvested after 0.5, 1, 3, 24 or 48 hours of incubation prior to staining. Data expressed as mean of at least triplicate independent experiments, all performed with technical triplicate. Significance of response calculated relative to untreated cells (UT). **** $P < 0.0001$ (1-way ANOVA with Dunnett's multiple comparisons testing). Vertical dashed lines on the X-axes indicate the transition between IFN-β and IFN-β FLETVR treatments.

FIGURE 5. IFN-β FLETVR variant induces reduced STAT1 phosphorylation compared to IFN-β. (A) L929 cells were treated with either 1 ng/mL or 5 ng/mL IFN-β or the IFN-β FLETVR variant for either 30 or 120 minutes. STAT1 phosphorylated at Y^{701}, total STAT1 and actin were detected in whole cell lysates. This result is representative of triplicate independent experiments. (B) Densitometry of Western blots; data from the triplicate independent experiments are represented as intensity of phospho-STAT1 relative to intensity of actin. Data expressed as mean ± SD of triplicate independent experiments. Significance relative to untreated samples (UT), ** $P < 0.01$, **** $P < 0.0001$ (2-way ANOVA with Tukey's multiple comparisons testing); significance relative to treatment with 1 ng/mL IFN-β for 30 mins, # $P < 0.05$, ### $P < 0.001$, #### $P < 0.0001$ (2-way ANOVA with Tukey's multiple comparisons testing).

FIGURE 6. Quantitative RT-PCR analysis of the response of L929 cells to treatment with IFN-β (■) or IFN-β FLETVR (▲) for 3 hours. The amplified target from each sample is relative to the levels of 18S in the same sample. All data is normalized to mRNA levels detected in untreated cells (●) and

expressed as mean ± SD of at least 3 independent experiments performed in technical triplicate. Significance indicated above data points compares treatment between IFN-β and IFN-β FLETVR at the same protein concentration (* $P < 0.05$, ** $P < 0.01$, *** $P < 0.001$, **** $P < 0.0001$ (2-way ANOVA with Sidak's multiple comparisons testing)). All IFN-β treated samples (as demonstrated by the bracket at the right-hand side of each graph) show fold induction significantly greater than the untreated samples (## $P < 0.01$ or less; 2-way ANOVA with Dunnett's multiple comparisons testing). Significant difference in fold induction between IFN-β FLETVR treated and untreated samples is indicated (## $P < 0.01$, # $P < 0.05$; 2-way ANOVA with Dunnett's multiple comparisons testing)).

FIGURE 7. Comparison of the biological responses of IFN-β and the IFN-β FLETVR variant on L929 cells. (A) The specific anti-viral activities (IU mg^{-1}) of IFN-β and IFN-β FLETVR is shown. Data shown are individual data points and mean ± SD of independent experiments. **** $P < 0.0001$ (Student's *t*-test). (B) Comparison of the anti-proliferative activity of IFN-β and IFN-β FLETVR variant. Cell proliferation was monitored over 72h in the presence of the indicated doses of either IFN-β or IFN-β FLETVR. Data shown is the 72 hr time point and is expressed as mean ± SD of triplicate independent experiments, performed in technical quadruplicate, analysed using 2-way ANOVA with Sidak's multiple comparisons test, **** $P < 0.0001$.

Figure 1

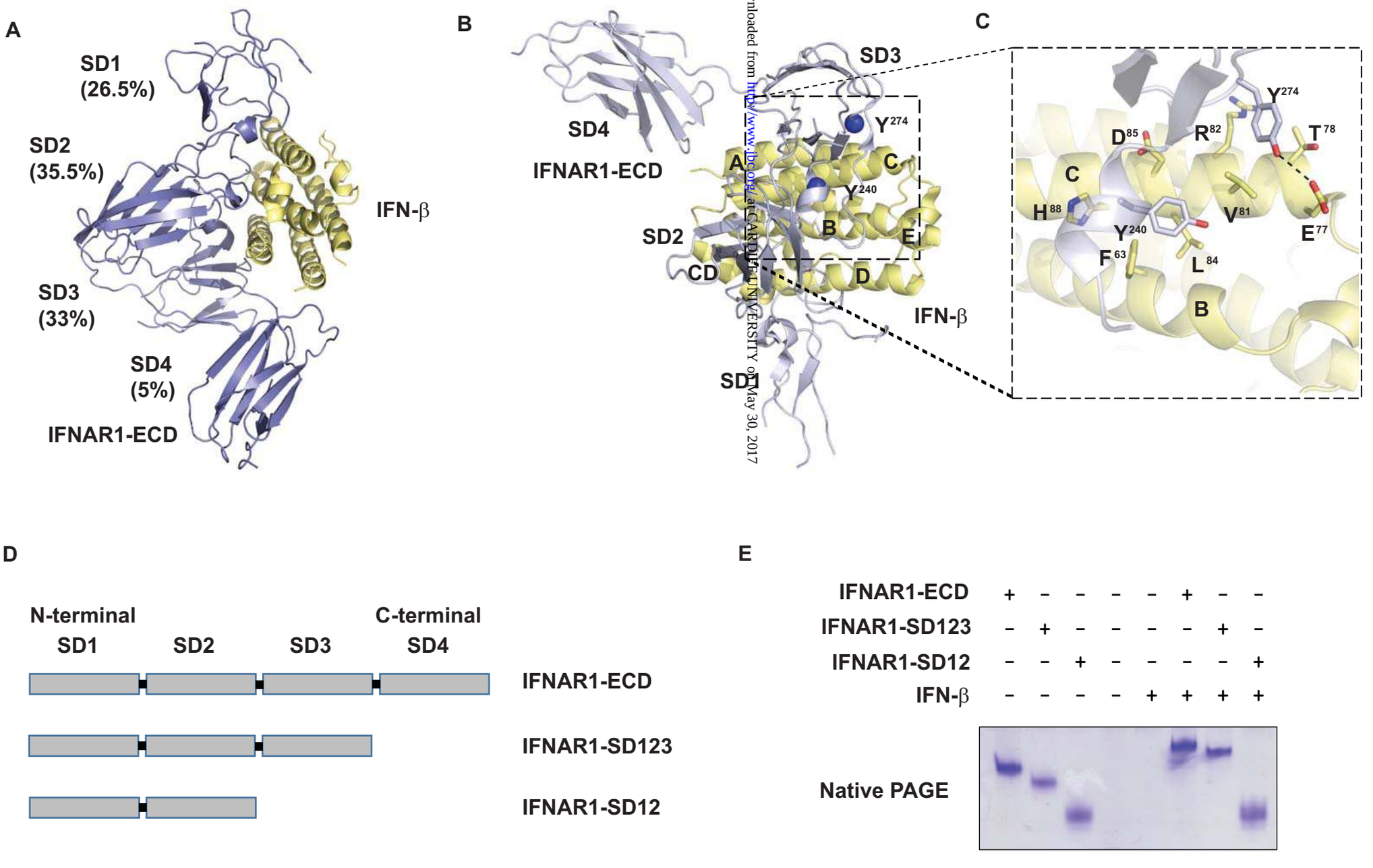

Figure 2

A

```
230  VLFRAQWLPGYSKSSSGSHSDEWKPIPTCANVQTTHCVFSQDTVYTGTFFL  280   IFNAR1
     --------------------A-------------------------------------------------------------   IFNAR1Y240A
     ----------------------------------------------------------------------------A-----   IFNAR1Y274A
     --------------------A-------------------------------------------------------A-----   IFNAR1YYAA
```

B

```
60   QNVFLVFRNNFSSTGWNETIVVRLLDELHQQ  90   IFN-β
     ------AA-----------------------------------------------   IFN-β FL63AA
     ----------------------------------AA-------------------   IFN-β ET77AA
     ------------------------------------AA-----------------   IFN-β VR81AA
     ------AA----------------------AA---AA-----------------   IFN-β FLETVR
```

C

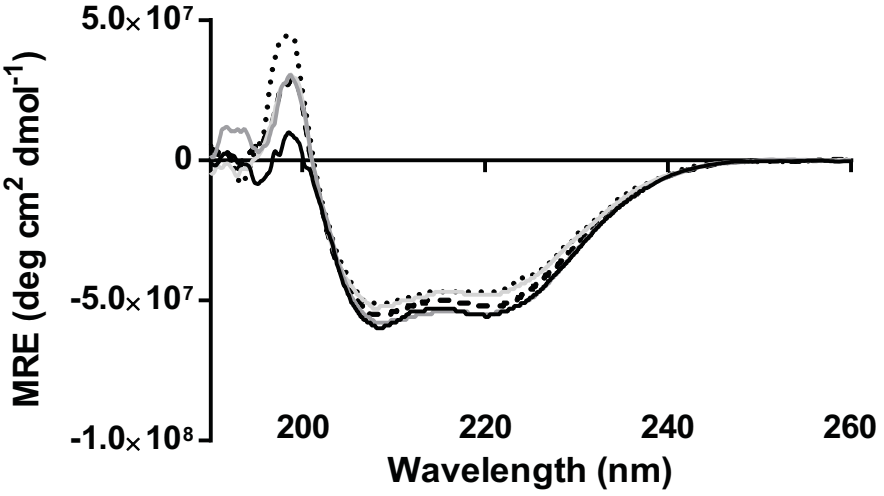

Figure 3

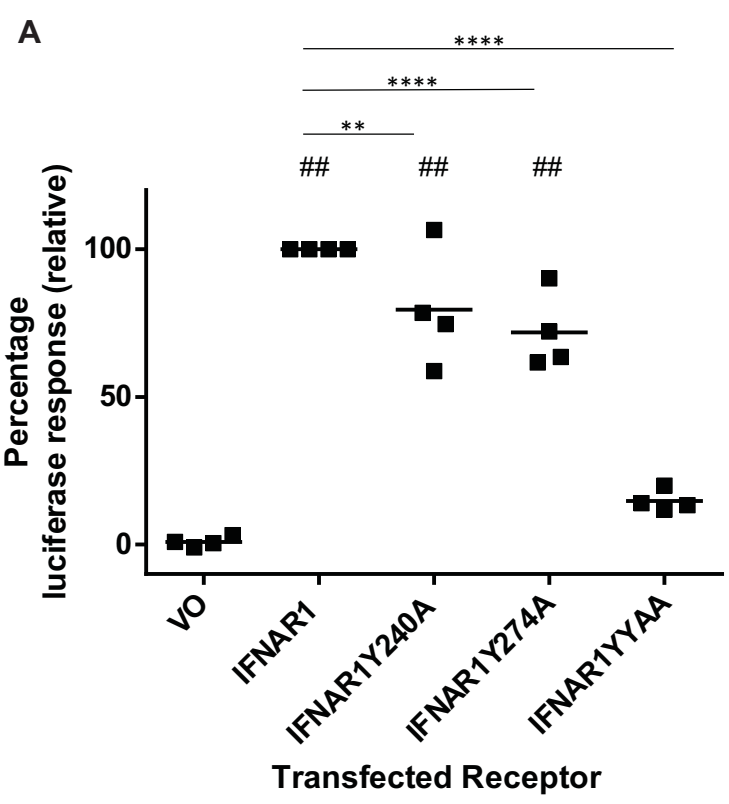

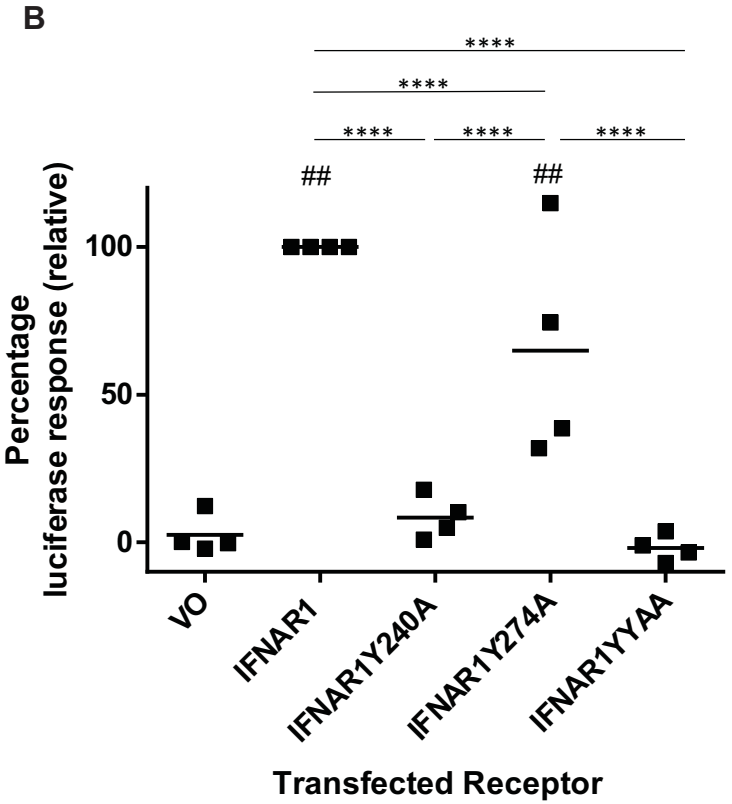

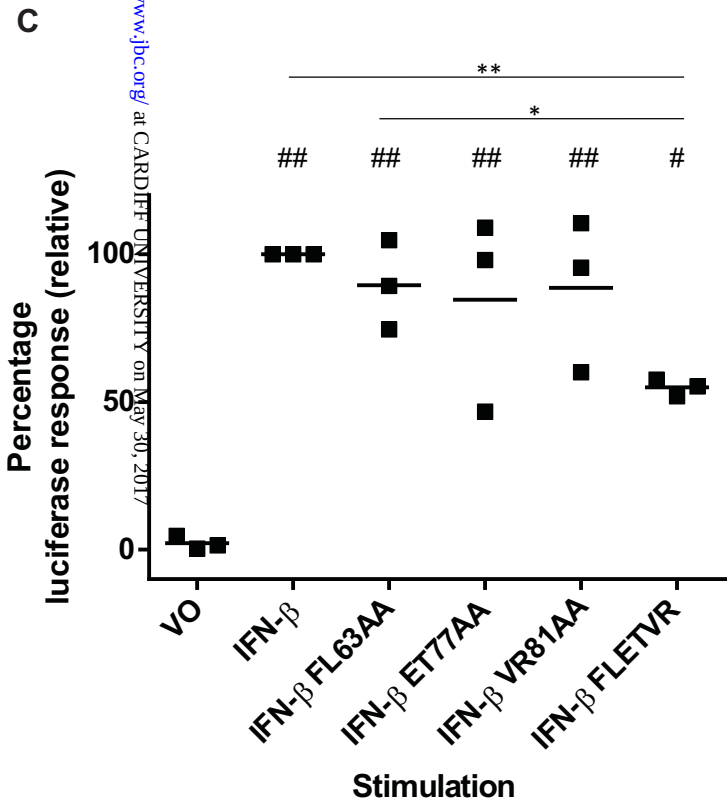

Figure 4

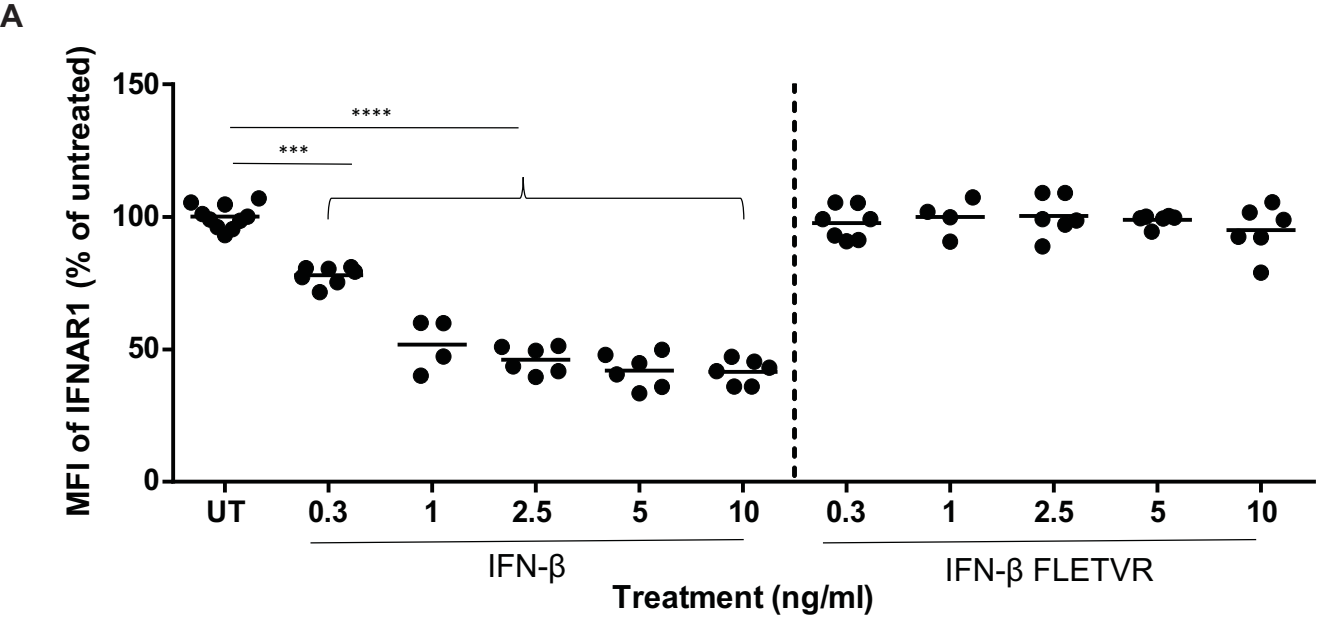

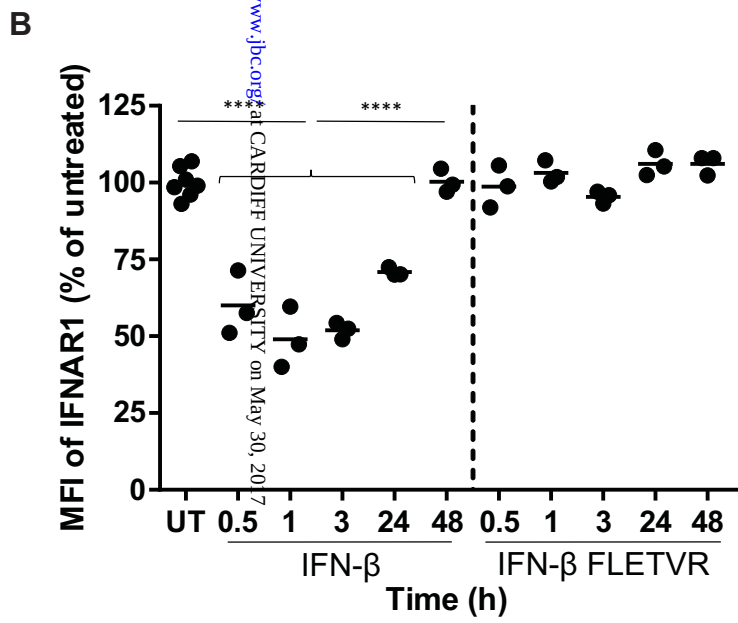

Figure 5

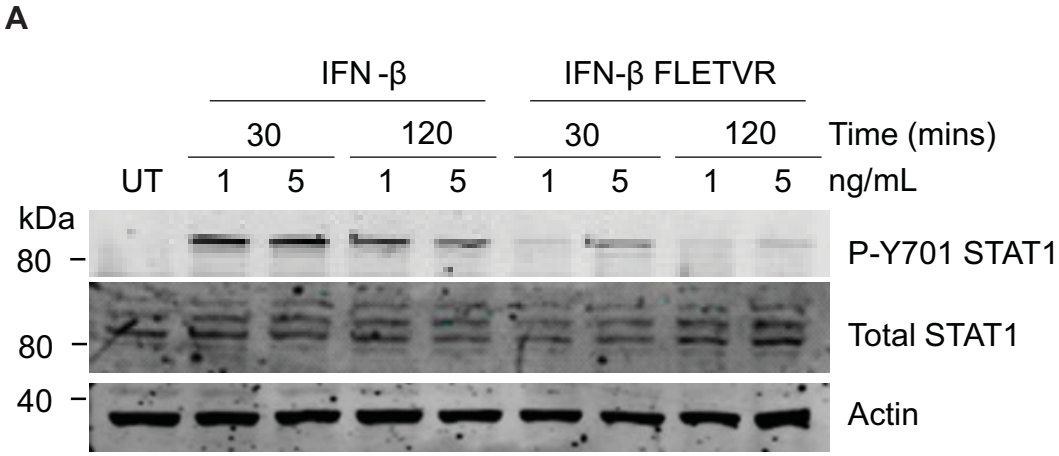

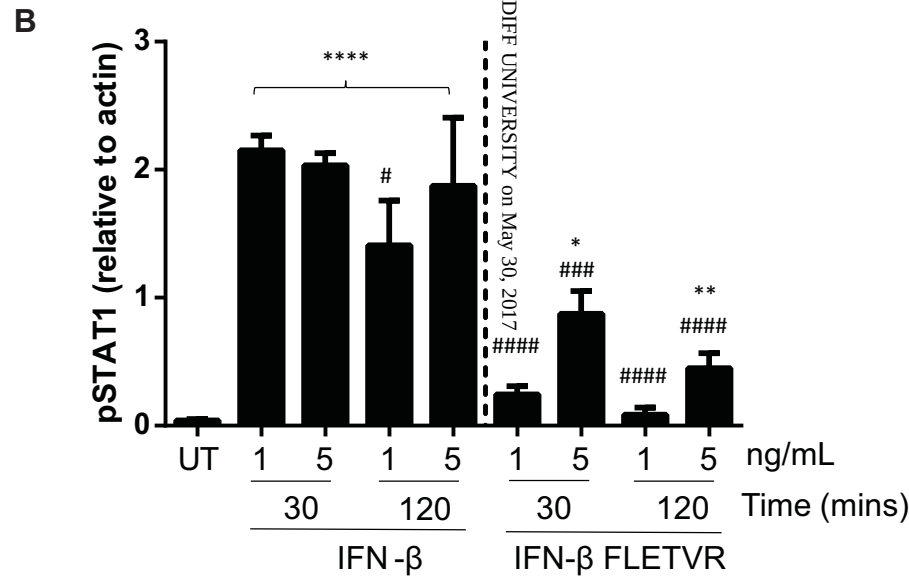

Figure 6

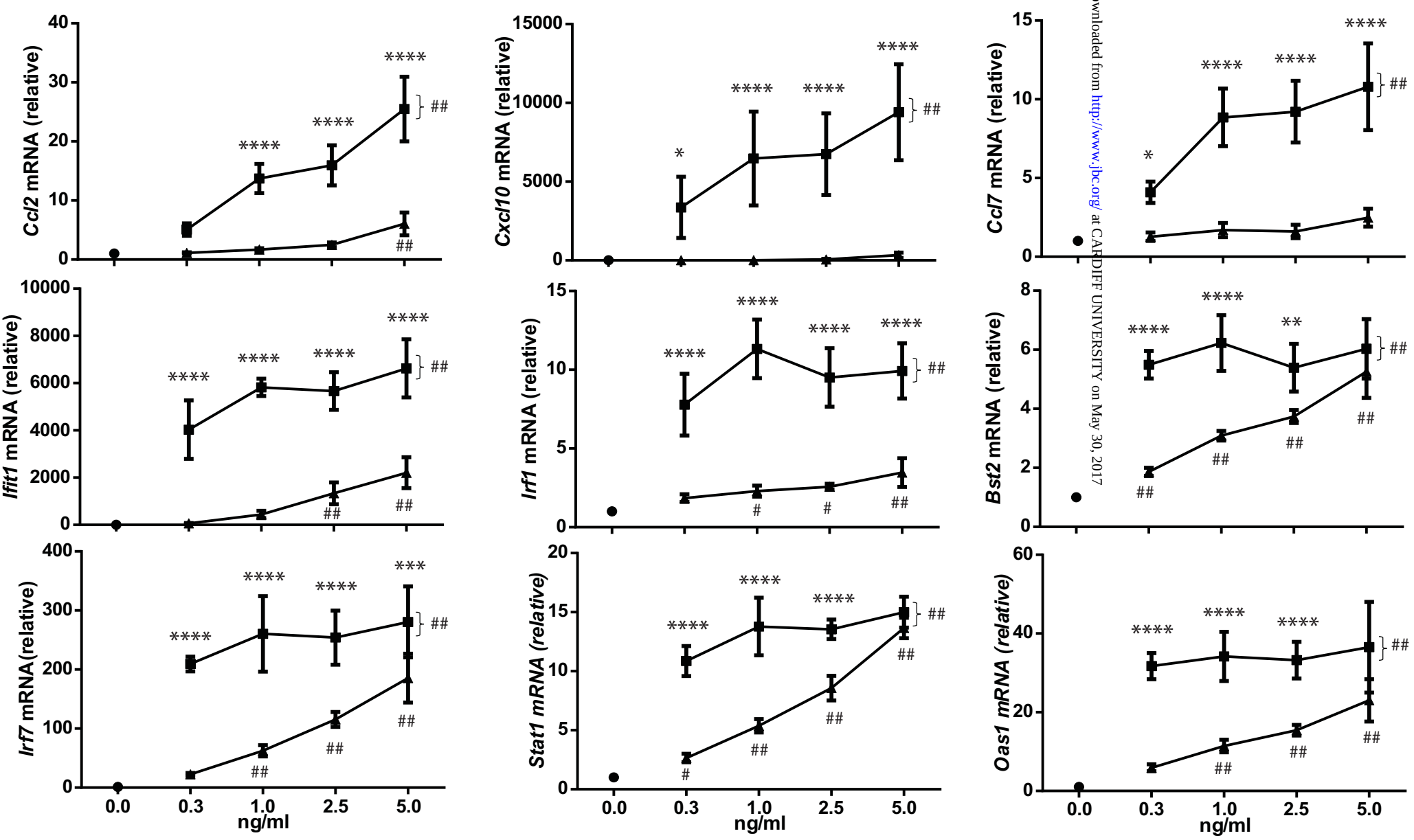

Figure 7

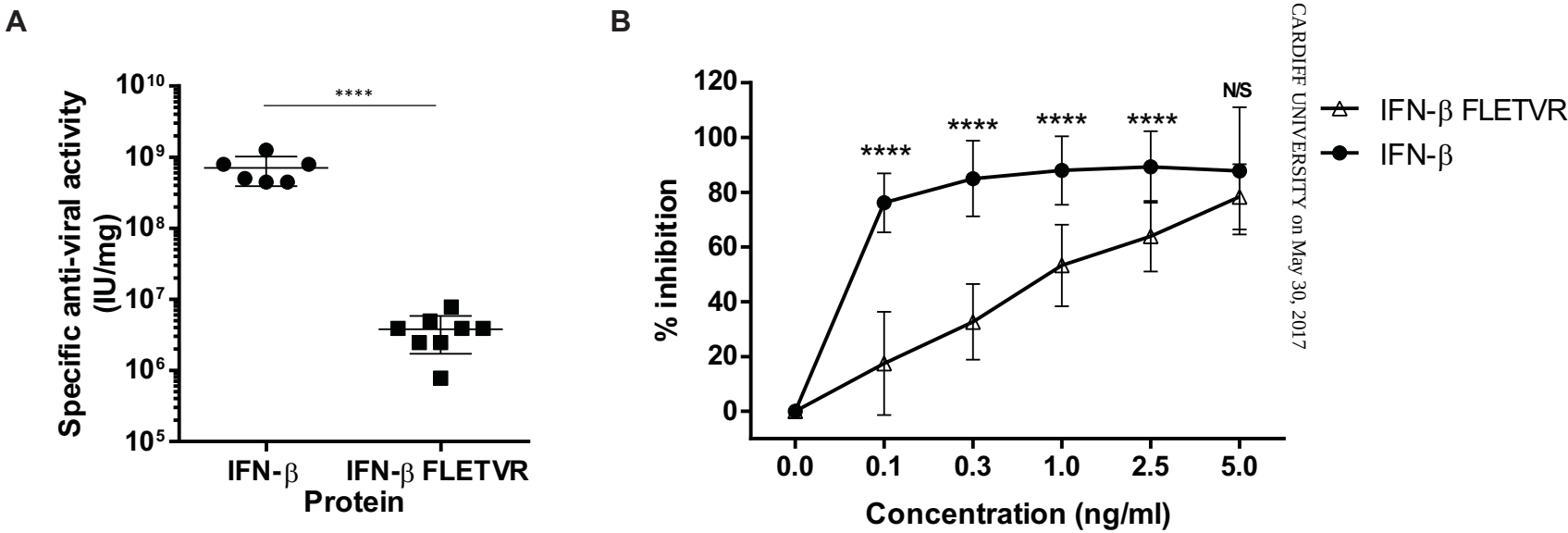

A hot-spot on interferon alpha/beta receptor subunit 1 (IFNAR1) underpins its interaction with interferon- β and dictates signaling

Nicole A. de Weerd, Antony Y. Matthews, Phillip R. Pattie, Nollaig M. Bourke, San S. Lim, Julian P. Vivian, Jamie Rossjohn and Paul J. Hertzog

J. Biol. Chem. published online March 13, 2017
